IEEE Access
Multidisciplinary | Rapid Review | Open Access Journal

Received April 29, 2020, accepted May 12, 2020, date of publication May 15, 2020, date of current version May 29, 2020.

Digital Object Identifier 10.1109/ACCESS.2020.2995069

Compact Size and High Gain of CPW-Fed UWB Strawberry Artistic Shaped Printed Monopole Antennas Using FSS Single Layer Reflector

AHMED JAMAL ABDULLAH AL-GBURI, IMRAN BIN MOHD IBRAHIM, MOHAMMED YOUSIF ZEAIN, AND ZAHRILADHA ZAKARIA, (Member, IEEE)

Centre For Telecommunication Research and Innovation (CeTRI), Faculty of Electronic and Computer Engineering, Universiti Teknikal Malaysia Melaka (UTeM), 76100 Durian Tunggal, Melaka

Corresponding author: Ahmed Jamal Abdullah Al-Gburi (engahmed_jamall@yahoo.com)

ABSTRACT This study proposed the use of coplanar waveguide Ultrawide-band strawberry artistic shaped printed monopole (SAPM) antenna with a single-layer frequency selective surface (FSS) as the metallic plate to improve the gain of antenna application. The intersection of six cylinders is used to structure the strawberry artistic shaped radiating element, which leads to enhancing the antenna bandwidth. The proposed FSS reflectors used a 10 × 10 array with the unit cell of 6mm × 6mm in introducing a center-operating frequency. This study used the FR4 substrate with coplanar waveguide (CPW) fed to print the proposed antenna, which provided a wide impedance bandwidth of 8.85 GHz (3.05–11.9GHz) that covers the licensed Ultrawide-band. The proposed FSS transmitted a stop-band transmission coefficient, which is below −10 dB with the linear reflection phase over the bandwidth in the range from 3.05 GHz to 11.9 GHz. The UWB SAPM antenna with FSS reflector showed an improvement from 1.65 dB to 7.87 dB in the lower band and 6.3 dB to 9.68 dB in the upper band with an enhancement of 6.22 dB. The gain value is enhanced by the gaping between the antenna and FSS, which has an approximately constant gain response through the band, the gain is sustained among 7.87 dB to 9.68 dB. The total dimension of the antenna is 61mm×61mm×1.6 mm. The proposed antenna structure provides the directional and balanced far-field pattern, which is suitable for Ultrawide-band (UWB) applications and ground-penetrating radar (GPR) applications.

INDEX TERMS UWB SAPM antenna, FSS reflector, gain, reflection phase, FSS array, stop-band.

I. INTRODUCTION

Ultrawide-band (UWB) is a telecommunication technology, which is used in wireless communicating networking to reach high rate bandwidth connections using a low level of energy consumption. The UWB was initially designed for commercial radar. UWB technology has many functions, including wireless personal area networks (PAN) and consumer electronics. After its first success in the middle of the 2000s, UWB radio becomes a developing technology with exclusive smart structures such as radar, wireless communications, and medical engineering areas [1], [2]. Before the year 2001, UWB was essential in military applications. After the year 2002, the Federal Communications Commission (FCC) allows the commercial use of UWB bandwidth to the public. Moreover, the FCC allowed the use of the UWB spectrum, which is within 3.1 GHz and 10.6 GHz in America [3]. The low frequency of spectral density is ideal for short-range communications. However, this function requires high gain antennas, accompanied by extremely stable radiation properties [4].

The UWB electronic devices use planar antennas, predominantly monopole [5] and slot, [6], which are feeds by a coplanar waveguide (CPW) [7], [8], for the features such as compressed dimension, low profile and low production cost, and Ultrawide impedance bandwidth. Unfortunately, this type of antennas can cause severe impedance mismatch when they are placed near metallic surfaces. Moreover, low profile antennas transmit low frequencies, which have low gain and poor directivity [9]–[11]. Specific applications require UWB antennas with high directivities, such as ground-penetrating radar (GPR). The high antenna gains and the utmost radiation in the broadside orientation is able to improve the penetration of the transmitted electromagnetic (EM) wave from the GPR transmitting antenna. The improvement can enhance the mitigation of soil altitude by expanding the frequency

The associate editor coordinating the review of this manuscript and approving it for publication was Kwok L. Chung.

of the process. Besides that, the device should maintain wider operational bandwidth to improve the lateral resolution of GPR.

The gain and the directivity of printed UWB antennas are improved by FSSs. Besides that, FSSs can safeguard the electronics below them. The overall system compactness is developed when the FSS separates the antenna and thereabout the metal surfaces before placing the printed antenna nearby the metal surfaces. FSSs are metasurfaces that exhibit an instantaneous response created by the replication of a pre-designed cell element. They function as a derivative filter (also known as Spatial Filter) that allow electromagnetic waves to transmit (pass-band filter) or reflect them (stop-band filter) [12], The filtering frequency depends on the arrangement as well as radiating element size, shape, and type, as well [13]. Frequency selective surface can use the ultra-wide stop-band by way of reflectors for UWB antennas.

Furthermore, FSS is able to observe the reflected wave in safeguarding constructive interference at the antenna surface over the reflection characteristics. To achieve high gain and to improve the front-to-back ratio, several existing design techniques have been introduced into FSS metasurface design and presented as a metallic reflector such as Mu near-zero (MNZ) [14], metasurface metallic reflector [15], superstrate Anisotropic metasurface [16], etc. The three limitations of FSSs are their large size, narrow bandwidth, and difficulty of design. It is challenging to realize the wideband single-layer FSS exists in the literature. However, to get a UWB response, the multi-layer configuration is used.

There are many current studies on several multi-layer FSS designs for UWB applications [17]–[20]. A double FSS layer is presented in [17], which provides the bandwidth of 10.35 GHz in 3.05GHz–13.4GHz with a gain enhancement of 2 dB to 4 dB. However, the design is too bulky, and the gain variation is not stable through the UWB band, the level of complexity with the FSS reflector is also enhanced. Previous studies presented three-layer, four-layer, and five-layer FSSs structures in [18], [19], and [20], respectively. The multi-layer FSSs provide UWB response, but they have limited practical use in recent communication gadgets due to their mass, complexity, and high-cost.

The single substrate layer is used to build the FSS for its compactness, which has a broad frequency response. Moreover, single-layer FSS can be easily integrated into modern portable electronics and communication gadgets. Lately, Some UWB FSS single-layer reflectors are designed to deliver flat gain in the Ultrawide-band frequencies [21]–[24]. In [21], A multi FSS single layer reflector is presented, which provides the bandwidth of 8.5 GHz in 2.5GHz – 11GHz with a constant gain enhancement of 5.5 dBi. However, the design is too bulky and complicated with the size of 82.5 mm × 82.5 mm for the first single-layer reflector (FSS1) and 62.5 mm × 62.5 mm for the second layer reflector (FSS2). Abdulhasan [22] proposed to study the use of a single-layer FSS with CPW feed by modified the square-loop structure on the FR4 substrate with a dimension of 11mm × 11mm × 21.6 mm. The fractional bandwidth was 6.8GHz (3.8-10.6GHz) and 3.5 dBi of improvement gain. However, the gain was poor, and the large air gap is realized, Tahir [23] proposed a novel single layer FSS reflector to achieve the bandwidth of 9 GHz in 3GHz – 12GHz and the improvement gain of 4 dBi, with a large FSS unit cell of 14mm × 14mm. This reference [24] provides a circular monopole slotted antenna with FSS to obtain high wideband gain applications. The antenna with FSS has a wide bandwidth range of 10.5 GHz in 3.5GHz – 14GHz with the max gain of 5 dBi and the overall size of the antenna with the dimension of 64 mm × 56 mm × 1.6 mm.

This study used a compact frequency selective surface (FSS) reflector, which is printed on an FR4 single layer to achieve a stop-band characteristic over an Ultrawide-band frequency range from 3.05 GHz – 11.9 GHz. The structure of the FSS is simple and easy to simulate as follows: 1) the actual size of the proposed FSS is 6 mm × 6 mm × 1.6mm, and 2) the electrical dimensions of the cell-element is 0.15 λ_0× 0.15 λ_0 × 0.04 λ_0. A distance of half wave-length conforming to the center frequency about 7.5 GHz was selected for optimization. The proposed FSS reflector with 10 × 10 array size of 61mm × 61mm × 1.6mm was used as a CPW UWB antenna to obtain a significant-high average gain of 9.68 dB, which is close to flat gain variation in the whole UWB frequencies. The following is the structure of this paper: 1) subsection 2 presents the design configuration of the proposed antenna and FSS, including the variation height (S), numbers of the unit cell (N.C), equivalent circuit (EC), metallic FSS array reflector, and the effects of surface current distributions; 2) subsection 3 presents the finalized UWB SAPM antenna with FSS single layer reflector; and 3) subsection 4 summarizes the research conclusion.

II. DESIGN CONFIGURATION

The advantages of monopole antenna are low profile, simple design, and ease of integration into the circuit board. However, its low gain and narrow bandwidth are unsuitable for UWB and GPR application band.

This section discusses the configuration and design principle of the UWB SAPM antenna with an FSS reflector to increase of gain over an ultra-wideband frequency range. This study used CST Studio Suite®EM analysis software tool in designing and modeling work. Moreover, a parametric study of the proposed FSS cell element was conducted utilizing the ultra-wideband ranges of (3.05 – 11.9) GHz. The design and characteristics of the single-layer FSS were investigated as the Metallic plate array for UWB applications.

A. UWB SAPM ANTENNA DESIGN CONFIGURATION

Fig. 1(A) indicates the structure of the UWB SAPM antenna and Fig. 1(B) presents the arrangement of the UWB SAPM antenna with an FSS single layer reflector. The dimension of the SAPM antenna is W × L of 26 mm × 26 mm × 1.6 mm. The strawberry artistic radiated patch is made from six cylinders with the following structure: first three

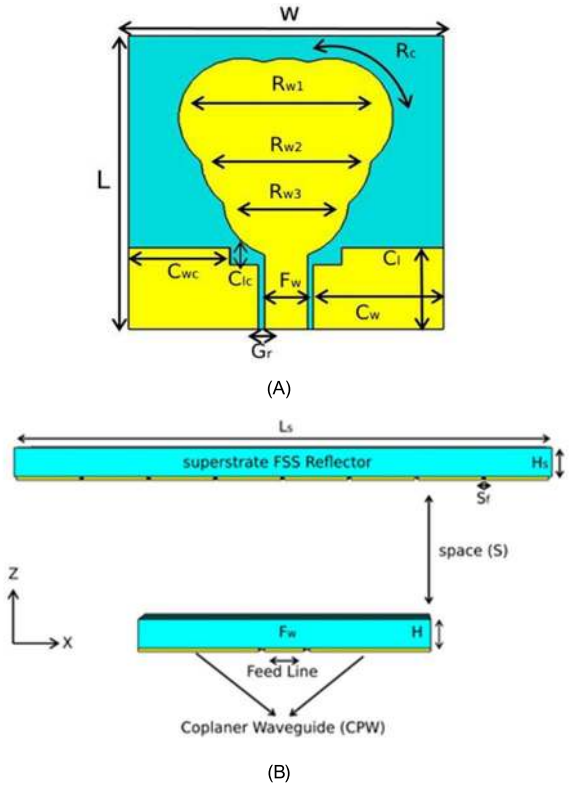

FIGURE 1. The structure of SAPM antenna with FSS single layer reflector: (A) SAPM antenna and (B) SAPM antenna with FSS reflector.

TABLE 1. The specification of the suggested SAPM antenna with FSS reflector.

Symbols in mm	Quantity
W	26
L	26
Rw1	17
Rw2	14.6
Rw3	10.8
Rc	6
Cl	7.5
Cw	11.15
Cwc	8.7
Clc	1.6
Fw	3.65
Gr	0.525
H	1.6
Hs	1.6
S	10
Sf	0.25

cylinders (RW1), second two cylinders (RW2), and third cylinder (RW3) that created the licensed ultra-wideband (3.05 – 11.9GHz) besides that, it helps to improve the impedance matching between the feed-line and the radiated patch. For the design of the antenna with coplanar-fed, the sides of the feed line were placed with two copper ground plane by a distance of Gr. Table 1 shows all the parameters. The equivalent cylindrical parameters of the proposed strawberry artistic patch were derived using Equation (1) [25]:

$$r = \frac{[2 \times R \times sin(\alpha) \times cos^3(\alpha)]}{\pi},$$
$$R = \frac{S_1}{[2 \times sin(\alpha)]}, \quad L = 2R(1) \tag{1}$$
$$f_L = \frac{C}{\lambda} = \frac{7.2}{[(L + r + p) \times k]} GH_z \tag{2}$$

Equation (2) is used by determining the area of the printed antenna and the corresponding cylindrical monopole antenna (CMA) to determine the decreased band edge (FL) of the suggested antenna. L is the height of the printed monopole antenna, r is indicating to the effective radius of a corresponding to the CMA, and the feed gap is stated by p. The rectification factor k is equal to 1.2, which is fixed for the dielectric substrate (FR4 material). This study selected the strawberry artistic patch shaped monopole antenna to function at the front side of the FSS array reflector as a radiator.

The proposed UWB SAPM antenna acts as a radiator, and it's designed on the FR4 substrate, which has a dielectric constant of 4.5 and dielectric loss (tan (δ)) of 0.02. Both the antenna and FSS layer have a similar thickness of the substrate (H=Hs=1.6mm) and materials (FR4 Substrate). The planned radiating structure has a rounded monopole antenna fed by 50 Ohm Coplanar Waveguide (CPW) and the FSS reflector with the dimensions of Ls. A set of uniform 10 × 10 unit cells is placed at the bottom of the single dielectric layer. The space between the FSS unit cell was carefully selected to obtain a constant impedance match. Besides that, the impedance of the monopole antenna is matched by means of a quarter wave-length (λ/4) transformer. The single-layer FSS reflector is covered by the UWB SAPM patch antenna at a space height (S).

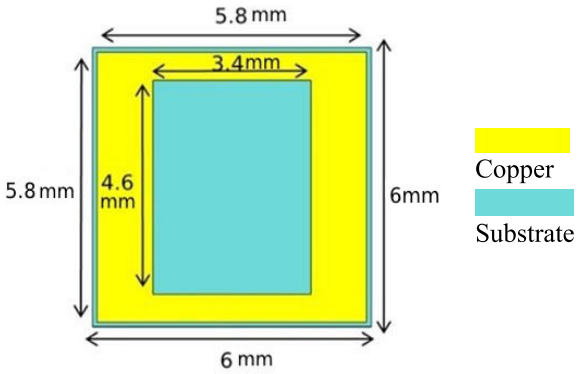

FIGURE 2. The structure of the suggested FSS.

B. FSS UNIT CELL DESIGN CONFIGURATION

FSS has planar periodic structures that are repeated in either one dimension or two dimensions. It has unit cells that are repeated consistently [13]. The resonance of FSS structures can be characterized by size, shape, and spacing between

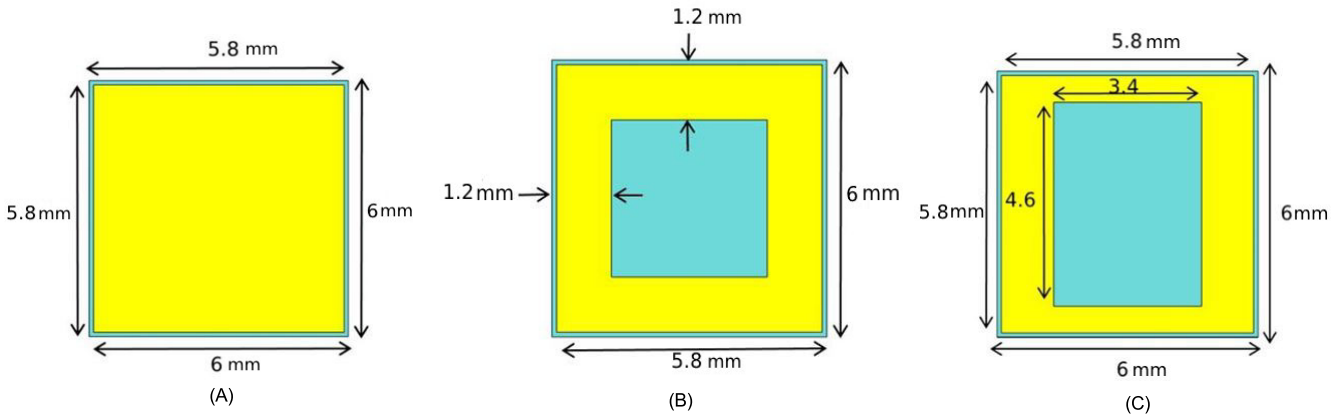

FIGURE 3. A parametric study of FSS cell unit: (A) conventional patch structure (CPS), (B) complementary loop structure (CLS), and (C) optimum square loop structure (OSLS).

the elements. They can reflect, transmit, or absorb the electromagnetic radiation. Besides that, the angle of incidence and polarization can affect the resonance. The dielectric that supports the FSS structures can also change the resonance. Generally, there are two types of FSS: 1) slot type that functions as a high pass filter; and 2) patch that works as a low pass filter. The formation of the suggested FSS unit cell is shown in Fig 2. The unit cell is printed using a square FR4 substrate with dielectric-constant (εr) of 4.5, loss tangent (tanδ) of 0.02, a thickness of 1.6 mm, and a dimension of 6 mm $\times$ 6 mm.

This study investigated the unit cell using CST-software to create an improved design of FSS that has a large bandwidth with a linear reflection phase. The first phase designed a unit-cell based on the conventional patch structure (CPS), which is further optimized through analytical modeling and simulations. The optimized design can obtain a stop-band at 9 GHz with a bandwidth of 8.5 GHz from 5.5 GHz to 14 GHz that achieves S21 < -10 dB, as shown in Fig. 4(A) The transmission coefficient (S21) is reduced at a lower and higher frequency. Moreover, the overall size of the CPS is 6 mm $\times$ 6 mm of copper. The second phase step adjusted the unit cell to obtain a complementary loop structure (CLS). Fig. 4(B) shows that the stop-band at 9 GHz becomes more significant with -48 dB, and the response of CLS has achieved a stop-band at 9 GHz of 9.7GHz bandwidth from 4.3GHz to 14GHz. However, the CLS response is still weak at the higher frequency, and it did not achieve the UWB stop-band (3.1-10.6) GHz. The final step decreased the length of the square loop to obtain an optimum square loop structure (OSLS), The bandwidth of the unit cell was improved to create a stop-band for the whole Ultrawide-band of bandwidth 8.85GHz from 3.05 GHz to 11.9 GHz as presented in Fig. 4(C).

Fig. 5. (A) shows the designate boundary and symmetry condition to clarify the behavior of the projected FSS. For the FSSs, the reflection phase is crucial for the improvement of antenna applications. In order to offer a phase reflection to the antennas, the phase of the FSS has to be linearly reduced. Fig. 5. (B) shows the proposed FSS that achieved a linearly declining phase from 3.05 GHz to 11.9 GHz.

C. EQUIVALENT CIRCUIT (EC)

The geometry of frequency selective surface (FSS) presented in Fig. 6(A), which is designed and investigated over an equivalent circuit (EC) of loop-FSS cell element. The equivalent circuit-model with chunked parts, such as inductance (LFSS) and capacitance (CFSS) of a square loop FSS cell element, is presented in Fig. 6 (B) contingent upon a transverse magnetic (TM) modes incident wave on the reflector, the columnar sectors facing up of loop perform a function as a CFSS. In contrast, the horizontal sectors perform a function as an LFSS. The variables of CFSS and LFSS are computed using equation (3) and equation (4) as assumed in [26], where Ce = 5.8 mm; Lh = 5.8 mm, Z1 = 0.6 mm; Z2 = 1.2 mm and g = 0.25 mm are estimated for the loop FSS cell element parameters as indicated in Fig. 6 (A).

$$\frac{X_{L_{FSS}}}{Z_0} = \omega L_{FSS} \frac{C_e}{L_h} \cos(\theta_i) F(L_h, 2Z_2, \lambda, \theta_i) \tag{3}$$

$$\frac{B_{C_{FSS}}}{Y_0} = \omega C_{FSS} = 4\frac{C_e}{L_h} \sin(\theta_i) F(L_h, s, \lambda, \theta_i)\varepsilon_e \tag{4}$$

$$F(L_h, W, \lambda, \theta_i) = \frac{p}{\lambda}\left[In\left(\cos\sec(\frac{\pi W}{2L_h})\right) + G(L_h, W, \lambda, \theta_i)\right] \tag{5}$$

$$G(L_h, W, \lambda, \theta_i) = \frac{1}{2} \times \frac{(1-\beta^2)^2[\left(1-\frac{\beta^2}{4}\right)(A_+ + A_-) + 4\beta^2 A_+ A_-]}{\left(1-\frac{\beta^2}{4}\right) + \beta^2\left(1+\frac{\beta^2}{2}-\frac{\beta^4}{8}\right)(A_+ + A_-) + 2\beta^6 A_+ A_-} \tag{6}$$

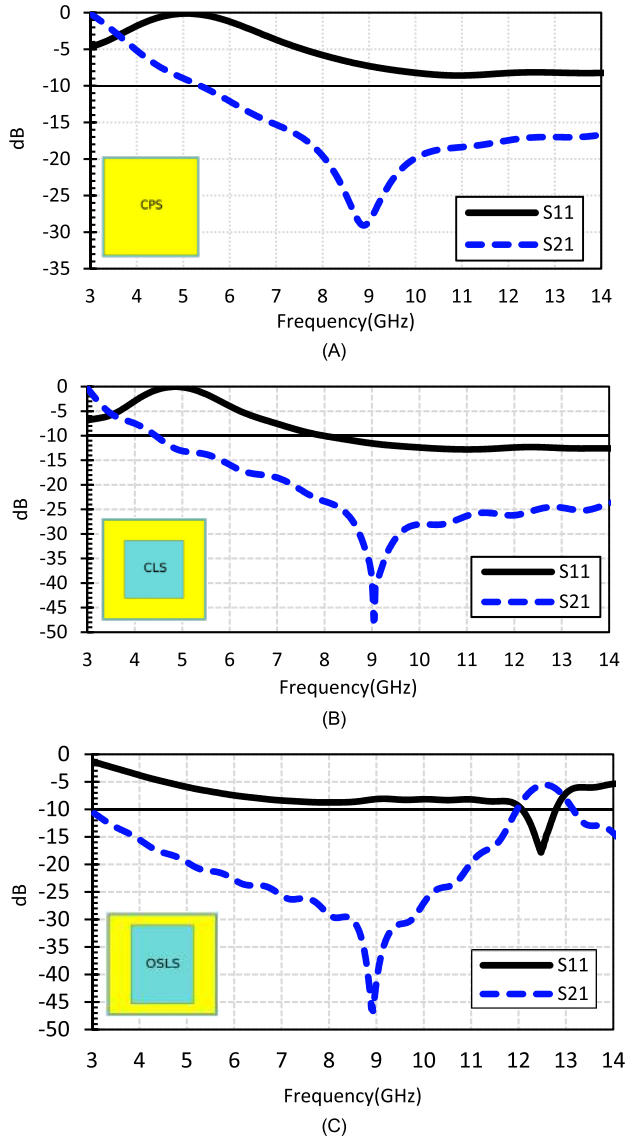

FIGURE 4. Reflection and transmission coefficients for the optimized steps of FSS structure: (A) conventional patch structure (CPS), (B) complementary loop structure (CLS), (C) optimum square loop structure (OSLS).

With,

$$A_{\pm} = \frac{1}{\sqrt{1 \pm \frac{2p\sin\theta}{y} - (\frac{pcos\theta}{y})^2}} - 1 \tag{7}$$

$$\beta = \sin(\frac{\pi w}{2p}) \tag{8}$$

Given that Z1 and Z2 are along with horizontal sectors and columnar sectors, accordingly, Z1 has employed for Transverse Electric (TE) modes, and Z2 is used for Transverse magnetic (TM) modes wave incidence for estimation of LFSS and CFSS. The Ce and w variables in eq.(5) up till eq.(8) need to be substituted by the favorable inputs characterized in eq.(3) and eq.(4) moreover, the value of parameters Ce, Z2 and g are maintained constant and designed using equivalent circuit (EC).

D. METALIC FSS ARRAY REFLECTOR

This study had successfully simulated the metallic FSS array reflector with different amounts of 1) unit cells (N.C), and 2) spaces(S), among the antenna and the metallic reflector after upgrading the transmission coefficient and reflection coefficient of the suggested FSS structure. Then, the UWB SAPM antenna was mounted on the FSS array reflector to obtain high gain and directional radiations over UWB frequencies. A comprehensive parametric study was carried out to determine the best values of its spaces from the antenna and the number of unit cells. The outcomes of these studies are presented next.

First, the influence of the space between the antenna and the metallic reflector on the Ultrawide-band is investigated within a parametric study of the reflection coefficient (S11) of the antenna for various amounts of "S" as displayed in Fig. 7(A). As predicted, the FSS unit cells influence the matching band of the antenna as when "S" increases, the antenna bandwidth also increases. Moreover, the effect of the "S" parameter on the gain performance of the antenna is depicted in Fig. 7(B), where the realized gain, over the Ultrawide-band, is computed for different amounts of "S" This indicates that the gain turns differently across the operational band, which can be defined by the fact that the phase change computed by S is a function of frequency. As in summary, we can conclude that the operating band and the value of the peak realized gain of the antenna are incredibly reliant on how far the antenna is from the metallic reflector.

In other words, the radiations from the antenna are reflected by the FSS, which is placed under the antenna (radiator). The Front-to-Back Ratio (F/B Ratio) and the directivity of the proposed UWB antenna are improved by the FSS that reflects waves in the phase with radiated waves by the antenna. When the frequency increases, the antenna's radiated wave close up FSS also grows. The growth of frequency causes the decline of reflected-waves for the supportive interference at the antenna plane. The designed reflection phase in Fig. 5(B), predicted a linear decrease in the reflection phase of the FSS. Hence, the reflected-waves for the supportive interference at the antenna plane can be controlled by the proposed FSS. When studying the condition of productive intervention, it is important to take note on the height among the FSS and the radiator using the following equation:

$$\varphi_{FSS} = -2\beta S = 2n\pi \quad n = \ldots -2, -1, 0, 1, \ldots \tag{9}$$

where φFss is the reflection phase by the FSS, S is the height among the FSS reflector and the radiator, and β is the propagation wave consonant in the open-space. When S is close to (λ /2), when lambda (λ) is the wave-length equivalent to the frequency at the reflected plane φfss turns to zero. afterwards, both sides of Eq. (1) are equal. The reflection phase of the FSS equals to zero at 5 GHz. The value of S is 10 mm (λ /2) to satisfy Eq. (9). This study conducted

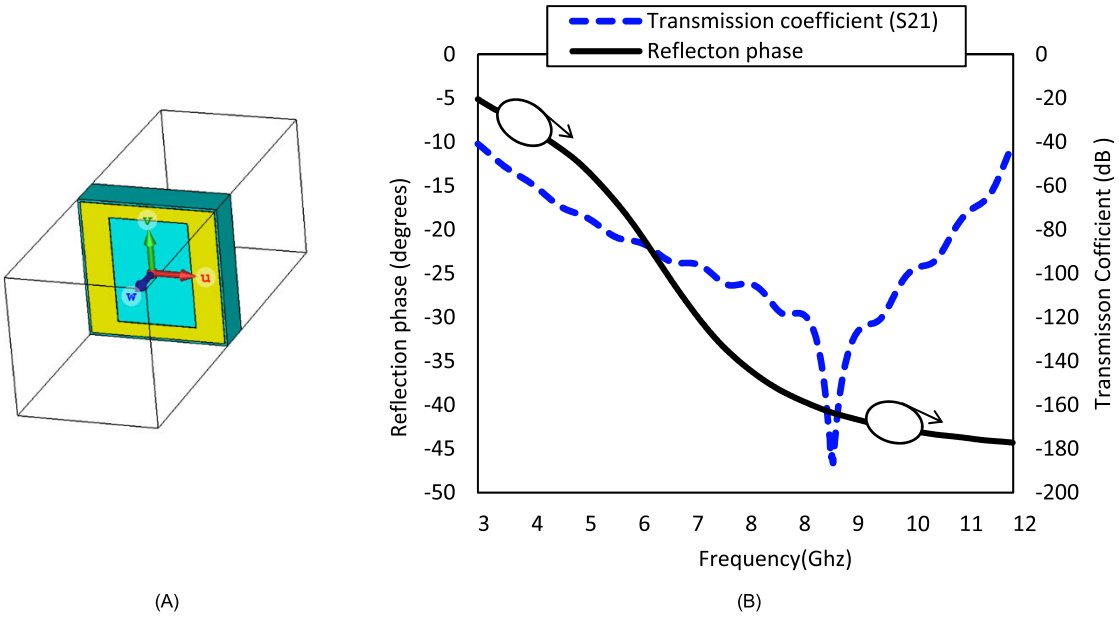

FIGURE 5. (A) Simulation of the unit cell and (B) predicted reflection phase and transmission coefficient (S21).

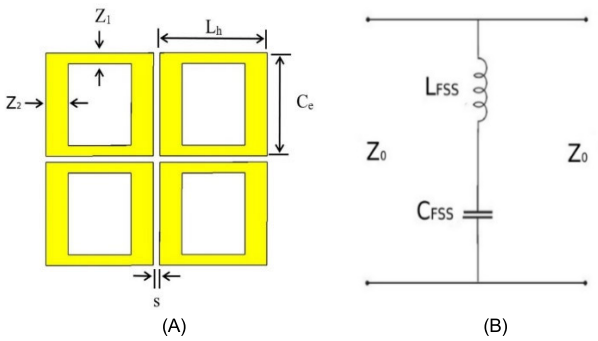

FIGURE 6. Loop FSS. (A) geometries (B) EC.

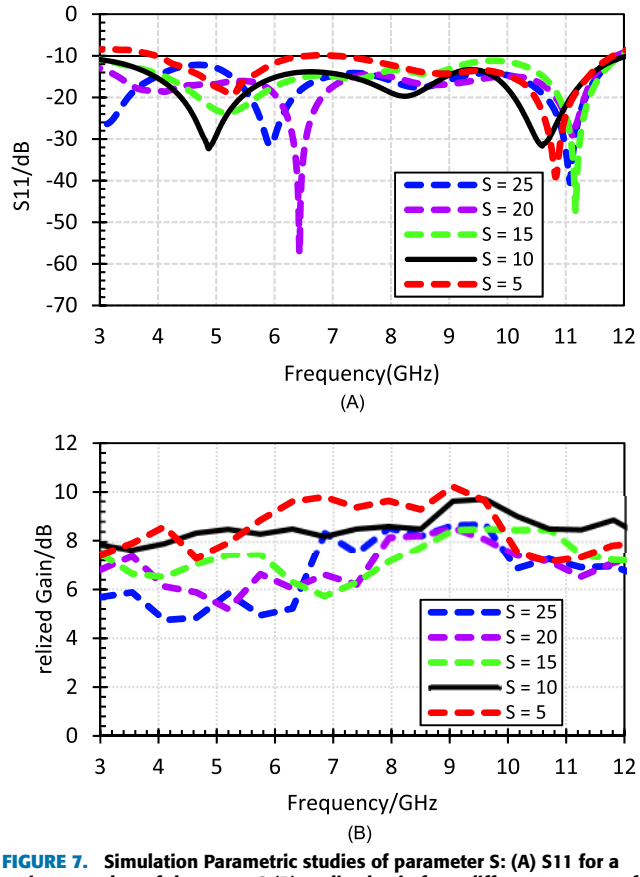

FIGURE 7. Simulation Parametric studies of parameter S: (A) S11 for a various number of the space S (B) realized gain for a different amount of the space S.

a comprehensive parametric study with different heights (S) of 5mm, 10mm, 15mm, 20mm, and 25 mm between the antenna and the reflector. The final stage uses the perfect height of 10 mm, which is (λ /4) that provides a comfortable response for the entire bandwidth.

The dimension of the FSS unit cells limits the overall size of the antenna. Hence, an in-depth analysis of the effects of the established FSS unit cell size on the given performance was achieved; the outcomes of this study are presented in Fig. 8, Fig. 8(A), which represents the reflection coefficient (S11) of the overall antenna with various amounts of unit cells (N.C), showing that the appropriating band of the antenna is primarily influenced by the part of the FSS that is placed immediately below the antenna, which means when FSS dimensions surpass those of the antenna. The antenna bandwidth becomes a standalone of the FSS dimension. The reflective performance of the FSS unit cell is figured by taking into account the unlimited FSS dimensions, which cannot be achieved where finite-size structures are needed. Nevertheless, by adding a large number of element cells, unlimited sizes can be approximated. Although the dimension of the FSS changes the radiation performance of the

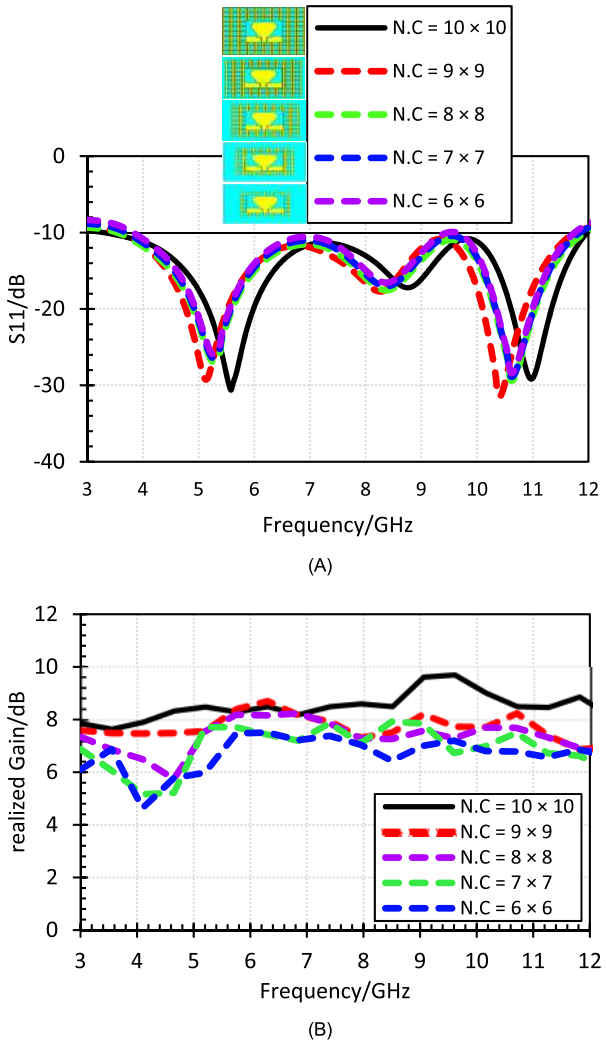

FIGURE 8. Simulation Parametric studies of parameter N.C: (A) S11 for a various number of unit cells N.C (B) realized gain for a different number of unit cells N.C.

antenna significantly, as presented in Fig. 8(B), into a parametric study of the antenna gain, showing that as the number of FSS unit cells increases, the gain also improves across the whole UWB band. Finally, the single-layer FSS reflector has 100 elements (10 × 10) array with better impedance-matching when compared with (9 × 9 = 81 elements), (8 × 8 = 64 elements), (7 × 7 = 49 elements) and (6 × 6 = 36 elements).

Fig. 9. Shows the present arrangement on the metallic sheet at various frequencies to study the reflection mechanism of the considered FSS structure with/without the antenna. However, it is revealed that the exited current flow is more energetic in the inner edge of the FSS unit cell, as displayed in Fig. 7(A). It can also be pointed out that the current is more saturated at the feed-line and lower side of the strawberry patch, as displayed in Fig. 7(B). The FSS reflector has a high current flow, and the surface current has an even arrangement of the antenna.

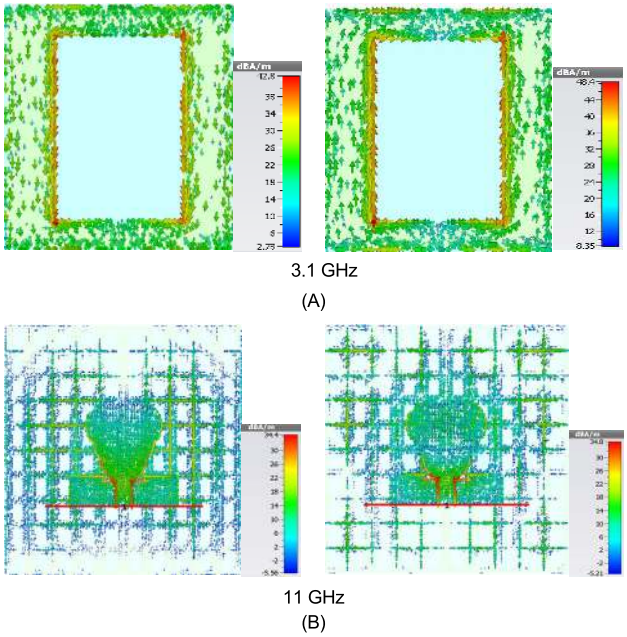

FIGURE 9. Simulated surface current at 3.1 GHz and 11 GHz for the following: (A) FSS unit cell only (left side operates at 3.1 GHz and the right at 11GHz), and (B) metallic FSS layer reflector with SAPM antenna (left size operates at 3.1 GHz and the right at 11GHz).

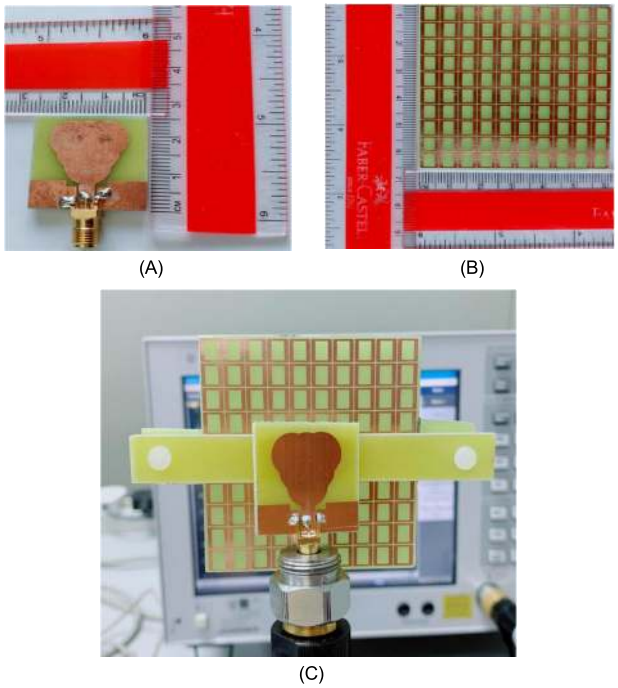

FIGURE 10. Fabricated prototypes for the following: (A) UWB SAPM antenna, (B) single-layer FSS reflector, and (C) UWB SAPM antenna with metallic single-layer FSS reflector.

III. UWB SAPM ANTENNA WITH METALLIC FSS SINGLE LAYER REFLECTOR AND MEASUREMENTS

This study had validated the simulation outcomes for both UWB SAPM antenna and UWB SAPM antenna with Metallic FSS single layer reflector in determining the characteristics of the fabricated strawberry artistic shaped printed monopole antenna. The finalized UWB SAPM

TABLE 2. Comparison of the related works.

References	Antenna Dimensions (mm)	Overall Dimensions (mm)	Electrical and physical dimensions Of FSS unit cell (mm)	Antenna Bandwidth/FBW (GHz)	Enhanced Gain (dB)	Number of the reflector layer	Number of the conductor layer
[17]	35 × 30 × 1.6	44 × 44 × 26.2	FSS1: $0.29\lambda_0 \times 0.27\lambda_0 \times 0.044\lambda_0$ (10.6 × 10 × 1.6) FSS2: $0.3\lambda_0 \times 0.3\ \lambda_0 \times 0.043\lambda_0$ (10.8 × 10.8 × 1.6)	126% (3.05-13.4)	5.5–8.5	Double	Double
[21]	50×50×1.524	FSS1: 82×82×22 FSS2: 62.5×62.5×22	FSS1: 0.19 λ_0 × 0.18 λ_0 ×0.034 λ_0 (8.25 × 8 × 1.524) FSS2: 0.14 λ_0 ×0.135 λ_0 ×0.034 (6.25 ×6.15×1.524)	125% (2.5–11)	FSS1: 8.0-9.0 FSS2: 7.5-8.5	Single	Single
[22]	31.9×30×1.6	31.9×30×29.6	0.27 λ_0 × 0.26 λ_0 × 0.039 λ_0 (11×11×1.6)	94% (3.8-10.6)	3.5-8	Single	Single
[23]	26×34×1.6	90×90×30	0.35 λ_0 × 0.35 λ_0 × 0.047 λ_0 (14×14×1.6)	120% (3-12)	5.5-8.9	Single	Single
[24]	-	64×56×18.2	0.34 λ_0 × 0.29 λ_0 × 0.05 λ_0 (11.5×10×1.6)	120% (3.5-14)	-1.0-5.0	Single	Single
This work	26×26×1.6	61×61×10	0.15 λ_0 × 0.12 λ_0 × 0.04 λ_0 (6×6×1.6)	118% (3.05-11.9)	7.87-9.68	single	Single

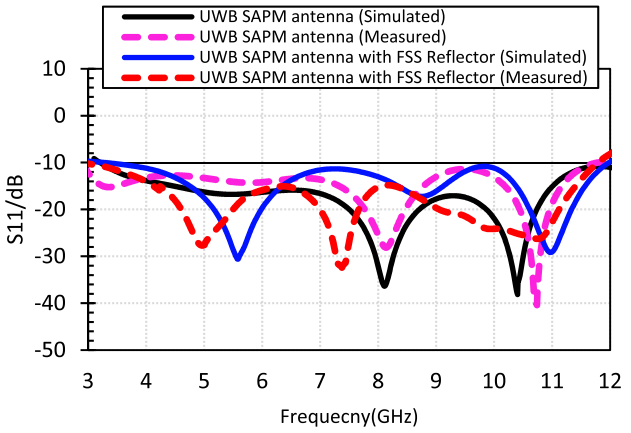

FIGURE 11. Predicated and Measured reflection coefficient (S11) of UWB SAPM antenna alone and with FSS single layer reflector.

antenna with metallic FSS reflector is printed on the FR4 substrate, as presented in Fig. 10. To assess the suggested antenna.

Fig. 11. compares the measured reflection-coefficient (S11) of the proposed prototype UWB SAPM antenna alone and with single-layer FSS reflector. The antenna with FSS obtains a bandwidth from 3.05 GHz to 11.9 GHz. The inaccuracies in construction have caused the differences between the theoretical and measured data, and more, due to the fabrication tolerances.

This study used a frequency swept RF signal from one of an anechoic chamber, namely source antennas, to illuminate the antenna AUT (antenna under test) to obtain the max gain over the frequency of UWB SAPM antenna with/without FSS reflector. Then, this study used the substitution method with the NSI far-field measurement system to calculate the gain of AUT in dB isotropic. The single-layer FSS reflector enhances the antenna gain across the entire UWB frequencies. Besides that, the antenna return loss is not affected by the reflector.

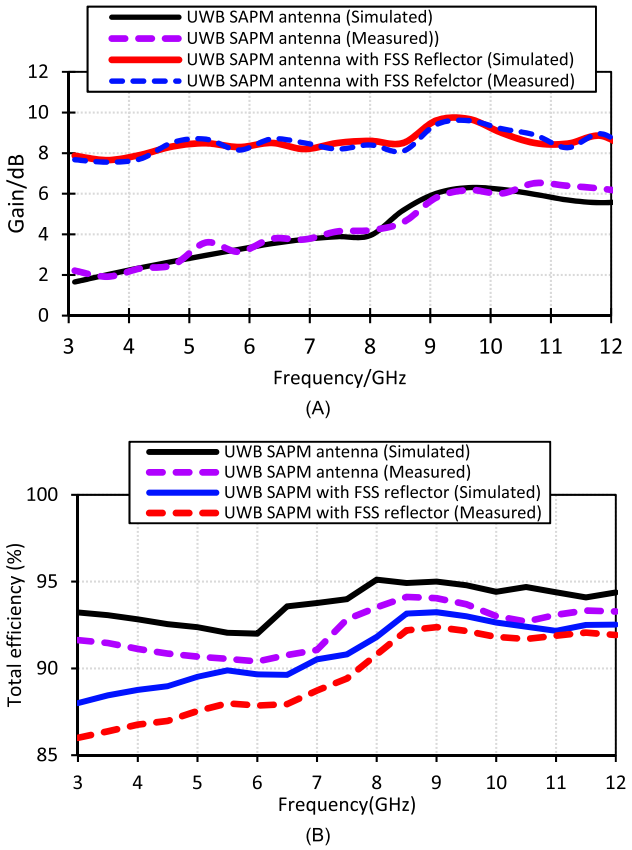

FIGURE 12. Predicated and Measured Gain (A) and total efficiency (B) of UWB SAPM antenna alone and with FSS single layer reflector.

There is a maximum increase of 6.22 dB in the antenna gain at 3.1 GHz, with a peak gain around 9.68 dB at 9.64 GHz. The maximum gain over UWB frequency is 9.68 dB for the antenna composite at 9 GHz. The gain and an antenna efficiency of the UWB SAPM antenna alone and with FSS single layer reflector are displayed in Fig. 12. The results confirm

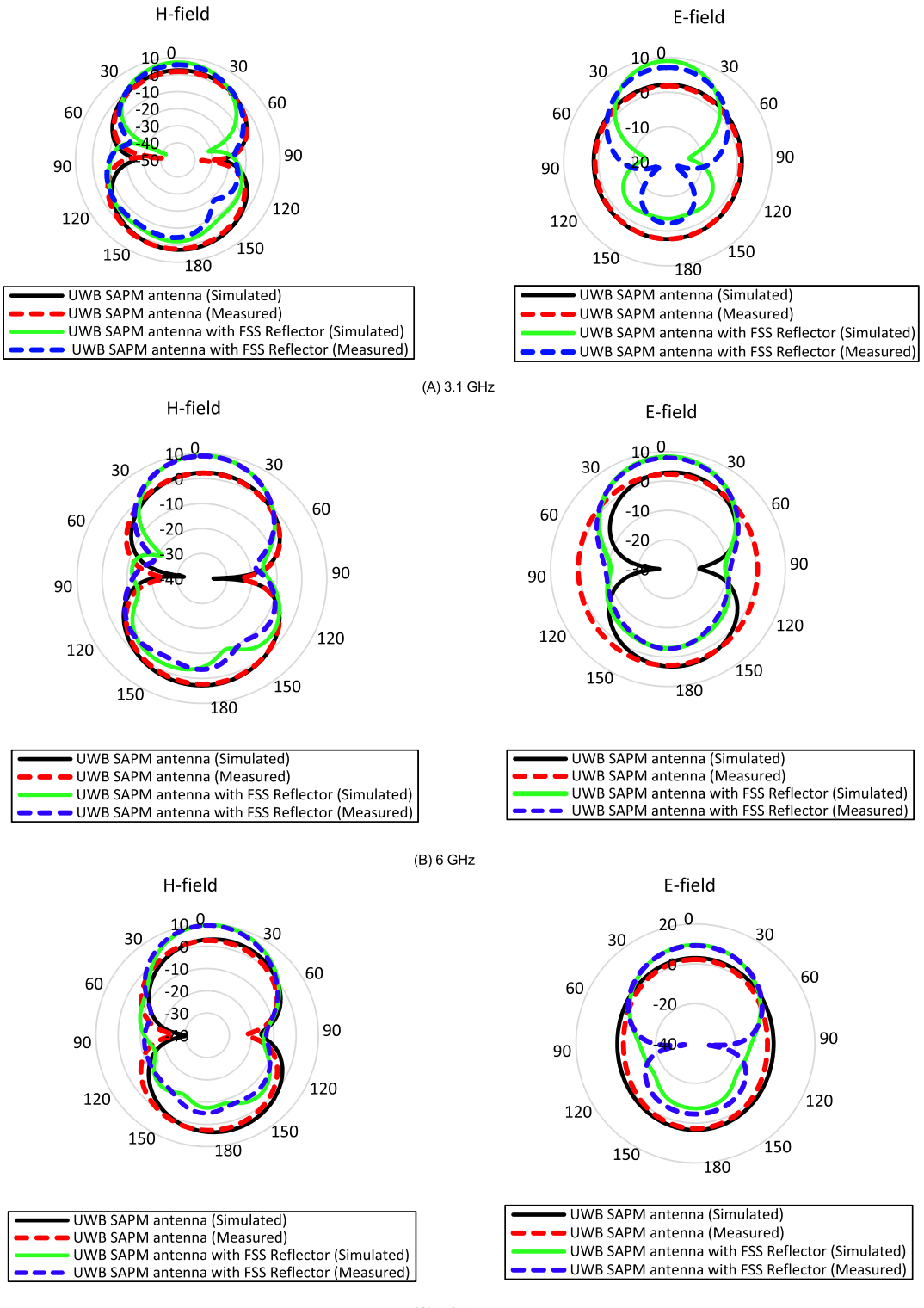

FIGURE 13. **Simulated and Measured E-field and H-field radiation pattern of UWB SAPM antenna with FSS single layer reflector at the following frequencies: (A) 3.1 GHz, (B) 6GHz, and (C) 9 GHz.**

that the measured UWB SAPM antenna achieves 94% of the total efficiency of the energy fed (−0.2dB), thence the measured UWB SAPM antenna along with FSS single layer reflector radiates 92% of Antenna efficiency with (−0.3dB).

Fig. 13. presents the measured far-field pattern at 3.1 GHz, 6 GHz, and 9 GHz on phi=0 and phi=90 planes. The antenna without FSS has an approximately Omni-directional pattern in H-plan and Figure-of-Eight polar pattern in E-plane,

as shown in Fig. 12. The directional antenna pattern is radiated by the metallic FSS reflector. The directivity of the antenna is improved by the application of frequency selective surface.

Finally, the comparison of related work is shown in Table 2. The main parameters of the UWB metallic FSS reflector loaded antenna with different layers are compared for this study for the following: single-layer, double-layer [17], [21]–[24] The study proposed the single FSS reflector that fulfills the operating characteristics of UWB due to its uncomplicated structure, low fabrication cost, compact size, and small flatness in the band. The proposed UWB SAPM antenna is compatible with the GPR application, and UWB application.

IV. CONCLUSIONS

A novel strawberry artistic shaped printed monopole (SAPM) antenna with a single-layer frequency selective surface (FSS) reflector as the metallic plate is presented in this article. Overall, the proposed SAPM antenna with an FSS reflector achieves high gain and directional radiation patterns. The electrical dimensions of the FSS structure are $0.15\lambda_0 \times 0.15\lambda_0 \times 0.04\lambda_0$, where λ_0 relates to the wave-length corresponding to the center of operating-frequency of 7.5 GHz with the stop-band of 8.85 GHz from 3.05 GHz to 11.9 GHz. The single dielectric layer can be used for the FSS design in achieving the stop-band response over the entire UWB frequency. This study presented the enhancement of the gain ability of FSS in which the UWB antenna was enhanced from 1.65 dB to 7.87 dB. The Highest realized gain by the antenna is 9.68 dB at 9.64 GHz, and the total efficiency of about 92%. The compact and low profile of the whole antenna with FSS is beneficial for UWB application, and ground-penetrating radar (GPR).

ACKNOWLEDGMENT

The author would like to express a sincere appreciation and thankfulness to the Centre for Telecommunication Research and Innovation (CeTRI) and Universiti Teknikal Malaysia Melaka (UTeM) through research grant PJP/2017/FKEKK/HI10/S01529 and provide the great facilities such IEEE Xplore digital library and research laboratory facility that made this research able to complete.

REFERENCES

[1] W. S. Yeoh and W. S. T. Rowe, "An UWB conical monopole antenna for multiservice wireless applications," *IEEE Antennas Wireless Propag. Lett.*, vol. 14, pp. 1085–1088, 2015.

[2] R. V. S. R. Krishna and R. Kumar, "A dual-polarized square-ring slot antenna for UWB, imaging, and radar applications," *IEEE Antennas Wireless Propag. Lett.*, vol. 15, pp. 195–198, 2016.

[3] S. Kim, Y. Kim, X. Li, and J. Kang, "Orthogonal pulse design in consideration of FCC and IEEE 802.15.4a constraints," *IEEE Commun. Lett.*, vol. 17, no. 5, pp. 896–899, May 2013.

[4] A. Domazetovic, L. J. Greenstein, N. B. Mandayam, and I. Seskar, "Propagation models for short-range wireless channels with predictable path geometries," *IEEE Trans. Commun.*, vol. 53, no. 7, pp. 1123–1126, Jul. 2005.

[5] J. Liang, C. C. Chiau, X. Chen, and C. G. Parini, "Study of a printed circular disc monopole antenna for UWB systems," *IEEE Trans. Antennas Propag.*, vol. 53, no. 11, pp. 3500–3504, Nov. 2005.

[6] E. S. Angelopoulos, A. Z. Anastopoulos, D. I. Kaklamani, A. A. Alexandridis, F. Lazarakis, and K. Dangakis, "Circular and elliptical CPW-fed slot and microstrip-fed antennas for ultrawideband applications," *IEEE Antennas Wireless Propag. Lett.*, vol. 5, pp. 294–297, 2006.

[7] Kwok L. Chung and S. Chaimool, "Triple-band CPW-FED L-shaped monopole antenna with small ground plane," *Microw. Opt. Technol. Lett.*, vol. 53, no. 10, pp. 2274–2277, 2011.

[8] S. Chaimool and K. L. Chung, "CPW-fed mirrored-L monopole antenna with distinct triple bands for WiFi and WiMAX applications," *Electron. Lett.*, vol. 45, no. 18, p. 928, 2009.

[9] J. Y. Siddiqui, C. Saha, and Y. M. M. Antar, "Compact dual-SRR-loaded UWB monopole antenna with dual frequency and wideband notch characteristics," *IEEE Antennas Wireless Propag. Lett.*, vol. 14, pp. 100–103, 2015.

[10] J. Liang, L. Guo, C. C. Chiau, and X. Chen, "CPW-fed circular disc monopole antenna for UWB applications," in *Proc. IEEE Int. Workshop Antenna Technol., Small Antennas Novel Metamater.*, vol. 2, Mar. 2005, pp. 505–508.

[11] A. M. Abbosh and M. E. Bialkowski, "Design of ultrawideband planar monopole antennas of circular and elliptical shape," *IEEE Trans. Antennas Propag.*, vol. 56, no. 1, pp. 17–23, Jan. 2008.

[12] J. D. Ortiz, J. D. Baena, V. Losada, F. Medina, R. Marques, and J. L. A. Quijano, "Self-complementary metasurface for designing narrow band pass/stop filters," *IEEE Microw. Wireless Compon. Lett.*, vol. 23, no. 6, pp. 291–293, Jun. 2013.

[13] R. Mittra, C. H. Chan, and T. Cwik, "Techniques for analyzing frequency selective surfaces—A review," *Proc. IEEE*, vol. 76, no. 12, pp. 1593–1615, Dec. 1988.

[14] K. L. Chung and S. Chaimool, "Broadside gain and bandwidth enhancement of microstrip patch antenna using a MNZ-metasurface," *Microw. Opt. Technol. Lett.*, vol. 54, no. 2, pp. 529–532, Feb. 2012.

[15] K. L. Chung and S. Kharkovsky, "Metasurface-loaded circularly-polarised slot antenna with high front-to-back ratio," *Electron. Lett.*, vol. 49, no. 16, pp. 979–981, 2013.

[16] K. L. Chung, S. Chaimool, and C. Zhang, "Wideband subwavelength-profile circularly polarised array antenna using anisotropic metasurface," *Electron. Lett.*, vol. 51, no. 18, pp. 1403–1405, Sep. 2015.

[17] S. Kundu, A. Chatterjee, S. K. Jana, and S. K. Parui, "A compact umbrella-shaped UWB antenna with gain augmentation using frequency selective surface," *Radioengineering*, vol. 27, no. 2, pp. 448–454, Jun. 2018.

[18] F. C. G. D. S. Segundo, A. L. P. D. S. Campos, and A. Gomes Neto, "A design proposal for ultrawide band frequency selective surface," *J. Microw., Optoelectron. Electromagn. Appl.*, vol. 12, no. 2, pp. 398–409, Dec. 2013.

[19] Y. Ranga, L. Matekovits, A. R. Weily, and K. P. Esselle, "A constant gain ultra-wideband antenna with a multi-layer frequency selective surface," *Prog. Electromagn. Res. Lett.*, vol. 38, pp. 119–125, 2013.

[20] A. Pirhadi, F. Keshmiri, M. Hakkak, and M. Tayarani, "Analysis and design of dual band high directive EBG resonator antenna using square loop FSS as superstrate layer," *Prog. Electromagn. Res.*, vol. 70, pp. 1–20, 2007.

[21] Y. Yuan, X. Xi, and Y. Zhao, "Compact UWB FSS reflector for antenna gain enhancement," *IET Microw., Antennas Propag.*, vol. 13, no. 10, pp. 1749–1755, Aug. 2019.

[22] R. A. Abdulhasan, R. Alias, K. N. Ramli, F. C. Seman, and R. A. Abd-Alhameed, "High gain CPW-fed UWB planar monopole antenna-based compact uniplanar frequency selective surface for microwave imaging," *Int. J. RF Microw. Comput.-Aided Eng.*, vol. 29, no. 8, 2019, Art. no. e21757.

[23] F. A. Tahir, T. Arshad, S. Ullah, and J. A. Flint, "A novel FSS for gain enhancement of printed antennas in UWB frequency spectrum," *Microw. Opt. Technol. Lett.*, vol. 59, no. 10, pp. 2698–2704, Oct. 2017.

[24] B. T. P. Madhav, A. V. Chaitanya, R. Jayaprada, and M. Pavani, "Circular monopole slotted antenna with FSS for high gain application," *ARPN J. Eng. Appl. Sci.*, vol. 11, no. 15, pp. 9022–9028, 2016.

[25] Z. Bocheng, L. Zhangfa, and L. Shizhi, *Novel Broadband Microstrip Antenna*, vol. 2. Boston, MA, USA: Girish Kumar and K. P. Ray, 1995.

[26] D. Ferreira, R. F. S. Caldeirinha, I. Cuinas, and T. R. Fernandes, "Square loop and slot frequency selective surfaces study for equivalent circuit model optimization," *IEEE Trans. Antennas Propag.*, vol. 63, no. 9, pp. 3947–3955, Sep. 2015.

AHMED JAMAL ABDULLAH AL-GBURI was born in Japan, Tokyo, in October 1989. He received the B.Sc. degree in software and computer engineering from the College of Computer Engineering, Damascus, Syria, in 2013, and the M.Sc. degree in electronic and computer engineering from Universiti Teknikal Malaysia Melaka (UTeM), Malaysia, in 2017, where he is currently pursuing the Ph.D. degree with the Faculty of Electronic and Computer Engineering (Telecommunication System).

His current research interests include analysis and antenna design, UWB antenna, high-gain monopole antenna, micro-strip patch antenna, electromagnetic band gap (EGB), split ring resonator (SRR), and frequency selective surface (FSS).

IMRAN BIN MOHD IBRAHIM was born in Kedah, Malaysia, in June 1976. He received the bachelor's, master's, and Ph.D. degrees in electrical engineering from UTM Malaysia, in 2000, 2005, and 2016, respectively. He is currently a Senior Lecturer with Universiti Teknikal Malaysia Melaka (UTeM). He has published more than 68 journals articles and conference papers. His research interests are antennas and propagations.

MOHAMMED YOUSIF ZEAIN was born in Baghdad, Iraq, in 1989. He received the B.S. from the Al Maarif University College (AUC) and the M.S. degree in electronic and computer engineering from Universiti Teknikal Malaysia Melaka (UTeM), Melaka, Malaysia, in 2017, where he is currently pursuing the Ph.D. degree in electronic and computer engineering. His research interests include antenna applications and 5G antenna.

ZAHRILADHA ZAKARIA (Member, IEEE) was born in Johor, Malaysia. He received the B.Eng. and M.Eng. degrees in electrical and electronic engineering from the Universiti Teknologi Malaysia, in 1998 and 2004, respectively, and the Ph.D. degree in electrical and electronic engineering from the Institute of Microwaves and Photonics (IMP), University of Leeds, U.K., in 2010. From 1998 to 2002, he was with STMicroelectronics, Malaysia where he worked as Product Engineer. He is currently a Professor with Microwave Research Group (MRG), Faculty of Electronic and Computer Engineering, University Teknikal Malaysia Melaka (UTeM), where he teaches Microwave Engineering, Antenna and Propagation, Electronic System, Communication Principles, Wireless Communications and Signal Processing. He has published more than 270 scientific articles in journals, proceedings and book-chapters. His research interests include variety of microwave devices development such as planar and non-planar microwave filters, resonators, amplifiers and antennas. He also investigates energy harvesting, sensor and data communications for interdisciplinary applications. He holds eight intellectual property rights and he has won several awards including gold medal during several research and innovation exhibitions at the national and international level, such as the UTeMEX 2012, 2013, and 2015, Malaysia Technology Expo (MTE 2012–2014 and 2016), ITEX 2016 and 2017, International Trade Fair Ideas Inventions New Products (iENA 2012) in Nuremberg, Germany, Seoul International Invention Fair (SiiF 2013, 2016, 2017 and 2019) in Seoul, South Korea. He is an active reviewer for prominent journals such as the IEEE Transactions on Microwave Theory and Techniques (MTT), the IEEE Sensor, IEEE Access, the IEEE Microwave and Wireless Components Letters (MWCL), IET Microwave, and Antennas and Propagation.